Neuron, *Volume 60*

Supplemental Data

The Neural Substrate of Spectral Preference in *Drosophila*

Shuying Gao, Shin-ya Takemura, Chun-Yuan Ting, Songling Huang, Zhiyuan Lu, Haojiang Luan, Jens Rister, Andreas S. Thum, Meiluen Yang, Sung-Tae Hong, Jing W. Wang, Ward F. Odenwald, Benjamin H. White, Ian A. Meinertzhagen, and Chi-Hon Lee

Supplemental Experimental Procedures

Comparative genomic analyses were carried out as previously reported (Odenwald et al., 2005; Yavatkar et al. 2008). Briefly, genomic regions (supplementary Figure 2) encompassing the *ort* and *HisCl1* genes from 12 *Drosophila* species were aligned using enchanced-BLAT program and analyzed using the *EvoPrinterHD* algorithms (Yavatkar et al. 2008). *Drosophila melanogaster* nucleotide residues that are conserved in at least 11 *Drosophila* species were highlighted with bold uppercase letters (supplementary Figure 2). Conserved regions (C1-C4 in *ort* and C1-C2 in *HisCl1* genes; underlined in supplementary Figure 2) were assigned by manually clustering the MCSs and excluding the coding regions.

Transgene constructions

Ort and *HisCl1* promoter fragments were PCR amplified from genomic DNA of wild-type Oregon-R flies and were used to generate various *ort* promoter-Gal4, LexA::VP16 and *HisCl1-Gal4* constructs (Figures 1, 6 and S3). Genomic sequences of *ort* and *HisCl1* genes are shown in Figure S2. Nucleotide sequences were verified by sequencing. Detailed maps are available upon request.

Cloning procedures are described as follows:

(1) For *ort*$^{C1\text{-}3}$*-Gal4* and *ort*$^{C1\text{-}3}$*-LexA::VP16*, the following PCR primers were used to amplify the ort promoter and to introduce restriction sites (Asp718 at 5' and BamH I, Not I, Xho I at 3'; underlined):

Forward: 5'-GAGCGGGTACCGCCAAACACAAGTAAAAAGTTTGCT-3';

Reverse: 5'-GGATTCTCGAGGCGGCCGCGGATCCTTTAATGTGAGCTCTTTCTG TGTGG-3'

The C1-3 fragment of the *ort* promoter was cloned into Asp718/Xho I sites of *pCaSpeR4* and the *Gal4* cDNA, isolated from pGaTB, was subsequently subcloned (via Bam HI and Not I site) into the resulting vector to generate *pCaSpeR4-ort*$^{C1\text{-}3}$*-Gal4*. The *LexA::VP16* cDNA was isolated from *pLot-LexA::VP16* (a generous gift from Tzumin Lee, UMass Medical School) and used to replace the *Gal4* cDNA in *pCaSpeR4-ort* $^{C1\text{-}3}$*-Gal4* (via Bam HI and Not I sites).

(2) For *ort*$^{C1\text{-}4}$*-Gal4*, the following primers were used to amplify the *ort* 3'UTR fragment, which contains the C4 conserved region, and to introduce Sal I and Not I restriction sites (underlined).

Forward: 5'-GTCGACTACGACGACTGTGCCCTGTA-3'.

Reverse: 5'-GCGGCCGCCCAACCGGCTGAGAAATAGT -3'.

The *ort* 3'UTR fragment was used to replace the *hsp70* 3'UTR in the *pCaSper4-ort*$^{C1\text{-}3}$*-Gal4* (via Sal I/Not I sites), resulting in *pCaSpeR4-ort*$^{C1\text{-}4}$*-Gal4*.

(3) For *ort*^{C1}*-Gal4*, the following primers were used to amplify the promoter fragment containing the C1 conserved region (Figure 6 and supplementary Figure 2) and the promoter fragment was then subcloned into the Asp 718 and Bam HI sites of *pCaSpeR4-ort*$^{C1\text{-}3}$*-Gal4* to replace the *ort*$^{C1\text{-}3}$ promoter fragment.

Forward: 5'-GAGCGGGTACCGCCAAACACAAGTAAAAAGTTTGCT-3'

Reverse: 5'-GGATTGGATCC(ATTTGAATTTAAAACGT)GCCCACTCGCCCAAGA-3'

(4) *ort*^{C2}*-Gal4* has been described previously as *ort-Gal4* (Hong et al. 2006).

(5) The *ort^{C3}-Gal4* was constructed in a similar fashion as that for *ort^{C1}-Gal4* except that the following primers were used to amplify the C3 region of the *ort* promoter:

Forward: 5'-GAGCGGGTACCTTGGTGAACTGTTCGTTCGT-3'

Reverse:5'-GGATTCTCGAGGCGGCCGCGGATCCTTTAATGTGAGCTCTTTCT GTGTGG-3'

(6) For *ort^{C1-3}-Gal4DBD*, the *ort* promoter C1-3 fragments were isolated from pCaSper4-ort^{C1-3}-Gal4 and subcloned into the EcoR I and Not I sites of *X11* (Luan et al., 2006). For *ort^{C2}-Gal4DBD*, the following primers were used to amplify the *ort* promoter fragment that contains the C2 conserved region (Figure 6A), and to introduce EcoR I and Not I restriction sites (underlined), and then subcloned into *X11* as described above.

Forward: 5'-GCGAATTCGTGGCAGGTCTCTGGGATTC -3'

Reverse: 5'-CCGCGGCCGCGACAGTTGGTGGCGAAC -3'

(7) For *ort^{C1-3}-Gal4AD*, the Gal4 activation domain (Gal4AD) was isolated from *CCAP-Gal4AD* (Luan et al., 2006) and subcloned into the Not I and Asc I sites of *ort^{C1-3}-Gal4DBD*, replacing the Gal4DBD fragment.

(8) *UAS-ort*, which contains the *ort* cDNA under the control of the *UAS* promoter, has been described previously (Rister et al., 2007).

(9) The Split-Gal4 enhancer trap plasmid *pP{y+, dVP16AD}* was constructed using a modified version of the VP16AD fragment from the original Split Gal4 system. The new fragment (dVP16AD), which is codon-optimized for expression in *Drosophila*, was used to replace Gal80 in the *pP{y+, Gal80}*(a generous gift from Drs. Christopher Potter and Liqun Luo, Stanford University). To hop *P{y+, dVP16AD}* into the *vGlut* locus, we injected the plasmid into the *yw, vGlut^{OK371}-Gal4* line (Mahr and Aberle, 2006) and screened for transgenic flies for yellow+. The transgenic flies were then crossed with *yw; UAS-EGFP; Elav-Gal4DBD* flies (Luan et al. 2006) and the progenies were screened for vGlut expression patterns. This method is similar to the "transposon swap" method described previously (Sepp and Auld, 1999) but uses direct injection to avoid making laborious genetic crosses.

Fly stocks

Fly stocks were reared in a standard medium supplemented with β-carotene (0.295g/L). All flies were raised at 25°C except those bearing *UAS-shi^{ts1}* and *Gal4* transgenes. The latter were reared at 18°C before experiments to avoid potential developmental defects. For behavioral experiments, flies were outcrossed for three generations to wild-type Canton-S (kindly provided by Dr. Howard Nash, NIH) to reduce potential effects from the genetic background.

The following driver lines were used for labeling neurons: (1) *w; ort^{C1-3}-LexA::VP16*; (2) *yw; vGlut-dVP16AD, ort^{C1-3}-Gal4DBD/CyO*; (3) *ort^{C1-3}-GAL4AD;; cha-Gal4DBD*; (4) *w;;ort^{C2}-Gal4/TM6B* (described as *ort-Gal4* in Hong et al. 2006); (5) *yw; ort^{C3}-Gal4*; (6) *yw; vGlut-dVP16AD/CyO; ort^{C2}-Gal4DBD/TM3*; (7) *w; HisCl1-Gal4/CyO; HisCl1-Gal4/TM6B*; (8) *w; vGlut-Gal4* (described as OK371-Gal4 in Mahr and Aberle, 2006) ; (9) *w; cha-Gal4* (Yasuyama et al., 1995); (10) *w; GAD1-Gal4* (a generous gift from Dr. Gero Miesenbock, Yale University; Ng et al. 2002); (11) *TH-Gal4*; and (12) *Ddc-Gal4* (Friggi-Grelin et al. 2003).

The following marker lines were used in combination with the driver lines described above to label neurons (1) *w;; LexAop-rCD2::GFP* (a generous gift from Dr. Tzumin Lee); (2) *yw; UAS-EGFP; UAS-mCD8GFP*; (3) *w; UAS-GFP^{nls}*; and (4) *yw;; UAS-mCD8GFP*.

To block the function of specific neuron subsets and assay the behavioral consequences, the *UAS-shi^{ts1}* lines (Kitamoto, 2001) were used in combination with the following driver lines: (1) *; ort $^{C1-4}$-Gal4*; (2) *; vGlut-dVP16AD, ort^{C1-3}-Gal4DBD/CyO*; (3) *ort^{C1-3}-GAL4AD;;cha-Gal4DBD*; (4) *w;Bl/CyO;ort^{C2}-Gal4/TM6B*; (5) *; ort^{C3}-Gal4*; (6) *yw; vGlut-dVP16AD/CyO; ort^{C2}-Gal4DBD/TM3*; (7) *w; L1L2-A*-Gal4 (Rister et al., 2007); (8) *w; Lot-shi^{ts1}*; *ort^{C1-3}-LexA::VP16*; (9) *Rh4-Gal4; Rh3-Gal4/CyO* (kindly provided by Dr. Claude Desplan, New York University).

For behavioral assays, the *Canton-S* strain was used as the wild-type control (kindly provided by Dr. Howard Nash, NIH). *sev^{E2}* and *NorpA^{36}* mutants (Bloomington Stock Center, Indiana) were used as negative controls. *HisCl1^{134}* mutants and double mutants *HisCl1^{134} ort^{1}* have been described previously (Hong et al. 2006). *ort^{US2515}* and *ort^{P306}*, which are strong hypomorphic alleles, were kindly provided by Dr. William Pak, Purdue

University). *ort^{1}*, which is null, was obtained from the Bloomington Stock Center (Gengs et al., 2002). These mutants were out-crossed to *Canton-S* and the presence of mutations was confirmed by PCR analyses.

To restore the function of neuron subsets and assay the behavioral consequences, the following stocks were used: (1) *; UAS-ort/CyO; ort^{US2515}*; (2) *w; ort^{C1-4}-Gal4/CyO ;ort^{1}/TM3*; (3) *yw; vGlut-dVP16AD,ort^{C1-3}-Gal4DBD/CyO; ort^{1}/TM3*; (4) *ort^{C1-3}-GAL4AD;; cha-Gal4DBD,ort^{1}/TM3*; (5) *w;; ort^{C2}-Gal4, ort^{1}/TM3*; (6) *yw; ort^{C3}-Gal4; ort^{1}/TM3*); (7) *yw; vGlut-dVP16AD; ort^{C2}-Gal4DBD, ort^{1}/TM3*; and (8) *L1L2-A-Gal4; ort^{1}/TM3*.

Confocal imaging of whole-mount brains

Whole-mount dissection, immunohistochemistry, confocal imaging (using a Zeiss LSM510 META and Plan Neofluar objective 40x/1.3), image deconvolution (Huygens Professional, Scientific Volume Imaging, Hilversum, Netherlands) and 3D image rendering (Imaris, Bitplane, Zurich, Switzerland) were all performed as described previously (Ting et al., 2005). The following dilutions of primary antibodies were used: mAb24B10, 1:100 (DSHB); mouse anti-FasIII 7G10, 1:25 (DSHB); mAbNC82, 1:25 (DSHB); mouse anti-Dlg 4F3, 1:50 (DSHB), mouse anti-Connectin C1.427, 1:50 (a generous gift from Dr. Robert White, Cambridge University); rabbit anti-Caps, 1:200 (a generous gift from Dr. Akinao Nose, Tokyo University); rabbit anti-GFP, 1:500 (Torrey Pines Biolabs, East Orange, NJ); rat anti-HA, 1:300 (Roche, Indianapolis, IN); and rat anti-mouse CD8a, 1:200 (Invitrogen, Carlsbad, CA). The secondary antibodies including goat anti-rabbit, rat or mouse IgG coupled to Alexa 488, Alexa 568, or Alexa 647 (Molecular Probes, Eugene, OR) were used at 1:200.

UV/Green Spectral Preference and Phototaxis Assays

The UV/Green spectral preference was carried out using a T-maze device made of transparent plexiglass (Lee et al., 2001). Two arms of the T-maze, fitted with transparent polystyrene vials (Fisher), were illuminated with either UV or green high-efficiency light-emitting diodes (LEDs 370 nm and 525 nm; Roithner Lasertechnik, Vienna, Austria) as described in Ting et al. 2007. Light intensity was calibrated at a distance of 13 cm to the light source (the distance from the center of the T-maze to the light source) using a Goldilux GRP-1 photometer. UV irradiance (in $\mu W/cm^2$) was measured using the GAP-1 probe. The illuminance of the green light (in Lx) was measured using the GLP-1 probe. The spectral composition, $S(\lambda)$, of the green light, determined by a spectroradiometer (Photo Research SpectraScan PR-670), was used to convert the illuminance reading to irradiance using the following formula: Irradiance = Illuminance x $\int S(\lambda)\, d\lambda$ / (6.83 x $\int S(\lambda)\, V(\lambda)\, d\lambda$); $V(\lambda)$ being the relative spectral sensitivity of the human eye.

Flies were pre-adapted to 50Lx (14 $\mu W/cm^2$) white light for at least one hour before testing. They were then knocked into a small compartment in the T-maze. After the adapting light was switched off and the test UV and green lights switched on, the flies now in an agitated state, were allowed to enter the vials illuminated by either test light. After each test, the flies in each vial were counted and the Performance Index (P.I.) calculated from the numbers choosing UV (N_{UV}) or green (N_G) light by the following formula: P.I. = ($N_{UV} - N_G$) / ($N_{UV} + N_G$). The few flies remaining in the center compartment were discounted. For each genotype, 8 trials (~30 flies of 3-7 days old per trial) were carried out for each point of the intensity ratio. Intensity-response curves were measured over eight orders of magnitude of a UV/green intensity ratio (10^{-5}-$2x10^4$). Green light intensity (in irradiance) was kept constant at 0.253 $\mu W/cm^2$ except at the maximum ratio (2176.7) at which it was reduced to 0.0363 $\mu W/cm^2$ to accommodate the intensity limit of the UV LED. The entire apparatus was housed in a temperature-controlled chamber. For tests using shi^{ts1}, the flies were pre-incubated for 5 min in the chamber at a non-permissive temperature (33°C) before behavioral assays were undertaken. The remaining experiments, including the shi^{ts1} controls, were carried out at a permissive temperature of 22°C.

Fast phototaxis towards UV or green light was measured using the same device as for the UV/green spectral preference assay except for the following modifications: (1) only one light source (UV or green) was switched on; (2) flies were adapted to either dark or 300 Lx (83 $\mu W/cm^2$) white light for 1 hr before testing.

Head Yaw Optomotor Response Assay

The head yaw optomotor assay has been described (Rister et al. 2007). To automate the measurement of head yaw, the following modifications were made. Images of fly heads were captured using an infrared camera (Sony) under infrared LED illumination and digitalized (at 30 frames/sec) using a frame-grabbing card from National Instruments (Austin, TX, USA). The images were processed in real-time or in batches using a pattern-matching program developed in house using the machine vision package from National Instruments. Head yaw angle was calculated by comparing the experimental images with a reference image taken before the experiments. For each genotype, ten flies 3-7 days of age were tested four times each.

Achromatic motion stimuli were provided by a high contrast pattern of four vertical black stripes (12^o) in a white background, printed with an HP Color Laserjet printer. The drum housing the striped pattern was rotated at a speed of $36\ ^o$/sec, first clockwise for 30 sec and then counterclockwise. Illumination was provided using a ring light. The light radiance of the black stripes and the white background were 0.003 and 0.03 $W/(Sr \cdot m^2)$, respectively.

Negative geotaxis assay

To identify potential motor defects, flies were tested for their ability to climb upward in the absence of visual cues. Briefly, flies (~20 per trial) were placed in a 30-cm long transparent plastic tube kept in an upright position. After being knocked to the bottom, flies were allowed to climb up the tube for 10 sec. Video images were recorded using an infrared camera (Sony) linked to a Windows-based PC and the position of each fly was tracked in real-time using a tracking program (Viewpoint). Flies were tested against a dark or a dim white light background (7 Lx, 1.9 $\mu W/cm^2$) with infrared illumination (870 nm). The distance each fly climbed in 8 sec was plotted. Approximately 300-400 flies were tested for each genotype.

Supplemental Figures and Legends

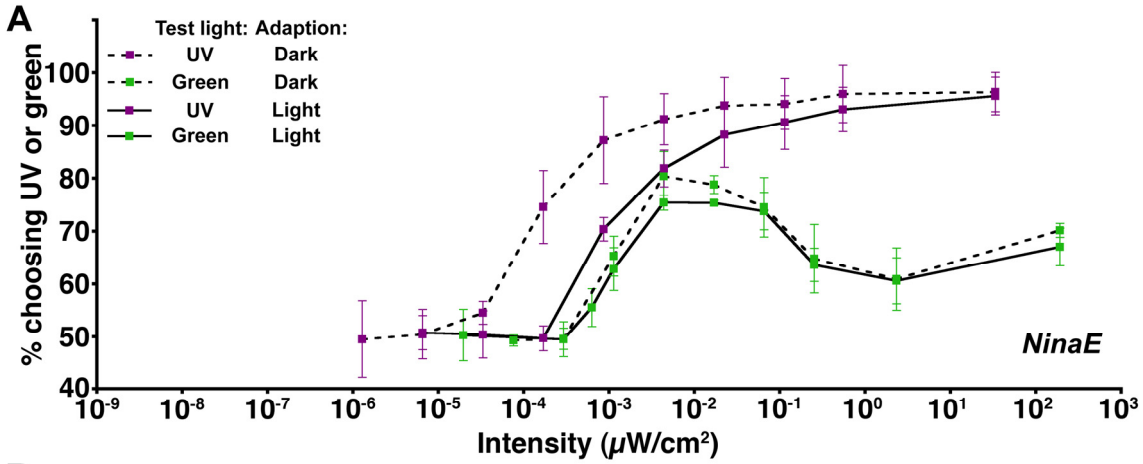

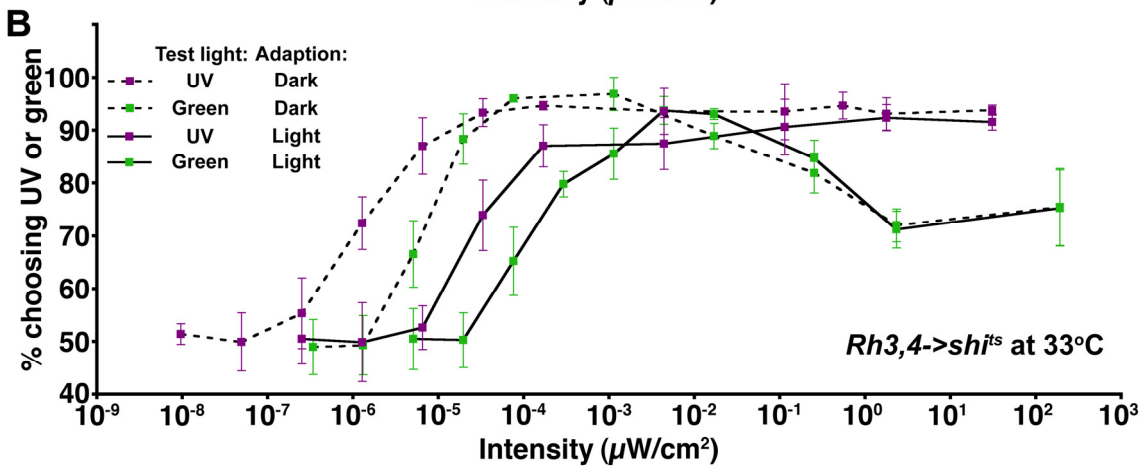

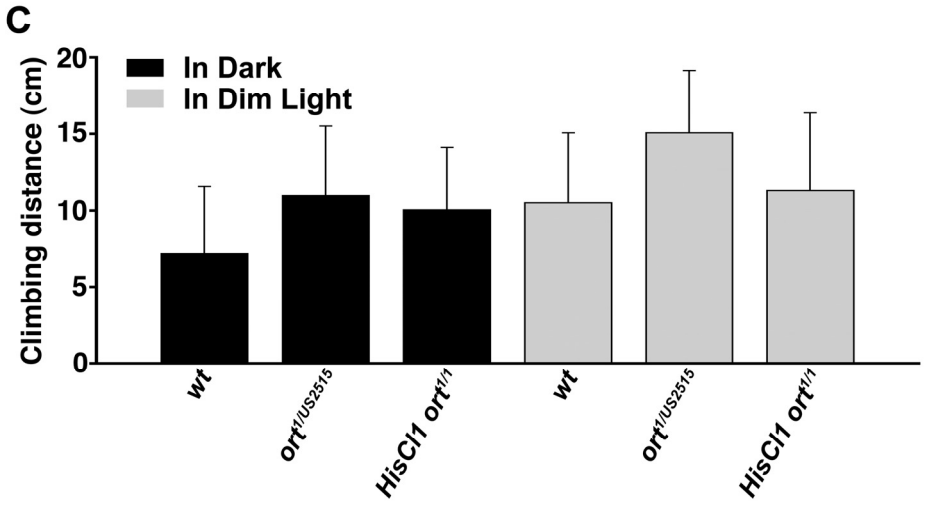

Figure S1. R1-R6 Photoreceptors Mediate Fast Phototaxis

(A-B) Mutants with defective R1-R6 or R7 functions were tested for fast phototaxis towards UV or green light as described in Figure 2A. The intensity-response curves were measured by recording the percentage of flies choosing UV or green light of various intensities over dark. Light intensity was shown as a logarithmic scale and error bars (standard deviations) represent the variations among trials.

(A) *NinaE* mutants, which lack the specific opsin for R1-R6, exhibited highly reduced phototactic responses to UV or green light. The intensity-response curves of *NinaE* mutants, when compared with those of wild-type (cf Figure 2A), were shifted to the right, and the maximal response towards green light failed to reach 100%.

(B) Inactivating R7s caused only a minor reduction in phototactic response towards UV. Flies carrying *Rh3,4->shi^{ts}* transgenes were tested for fast phototaxis at the non-permissive temperature. Their intensity-response curves resemble those of wild-type although the maximal response towards UV light was somewhat reduced under the light-adapted condition.

(C) *Ort* and *HisCl1 ort* double-null mutants exhibited no apparent motor defects. Motor functions of wild-type and *ort* and *HisCl1^{134} ort^{1}* double-null mutants were tested in negative geotaxis assays in darkness (black bars) or low light (grey bars) illumination. The average distance flies climbed in 8 sec was shown for each genotype. Error bars (standard deviation) represent variations among individual flies.

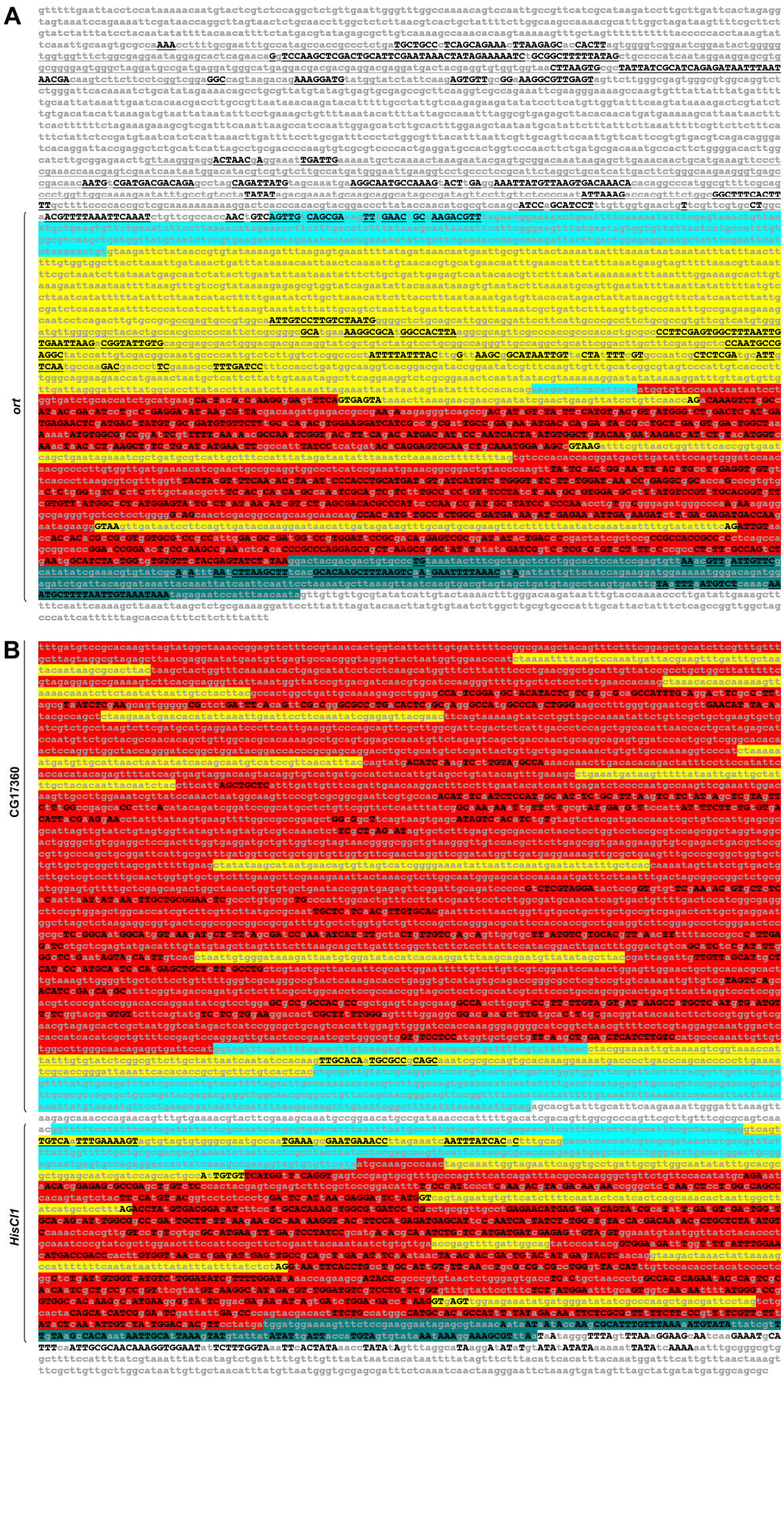
A
C1
C2
C3
C4
ort
B
CG17360
C2
C1
HisCl1

Figure S2. Comparative Genomic Sequence Analyses of the *ort* and *HisCl1* Loci

EvoPrinterHD analyses of the *histamine chloride channel 2 (ort)* (A), and *1* (*HisCl1*) (B), loci of 12 *Drosophila* species (see Experimental Procedures for details). Only the genomic sequences from *Drosophila melanogaster* are shown. Highly conserved nucleotides (shared by at least 11 species) are identified with bold uppercase letters. The transcribed sequences are labeled as follows: 5'UTR (light blue), protein-encoding sequence (red), 3'UTR (dark blue) and introns (yellow).

(A) Outside the protein-encoding regions, the conserved sequences of the *ort* gene are clustered in four regions, C1-C4 (underlined). C1 and C2 are located in the intergenic region and C3 in the first intron. The *ort* promoter region containing C1-C3 gives rise to cell-specific expression patterns. C4, located in the 3'-UTR, contains several potential binding sites for micro-RNA, but does not appear to affect cell-type specific expression.

(B) Two conserved regions, C1 and C2, were identified in the first intron of the *HisCl1* gene and the first intron of the neighboring gene, *CG17360*, respectively. The C2 region appears to be critical for driving glia-specific expression, which C1 alone fails to do (data not shown).

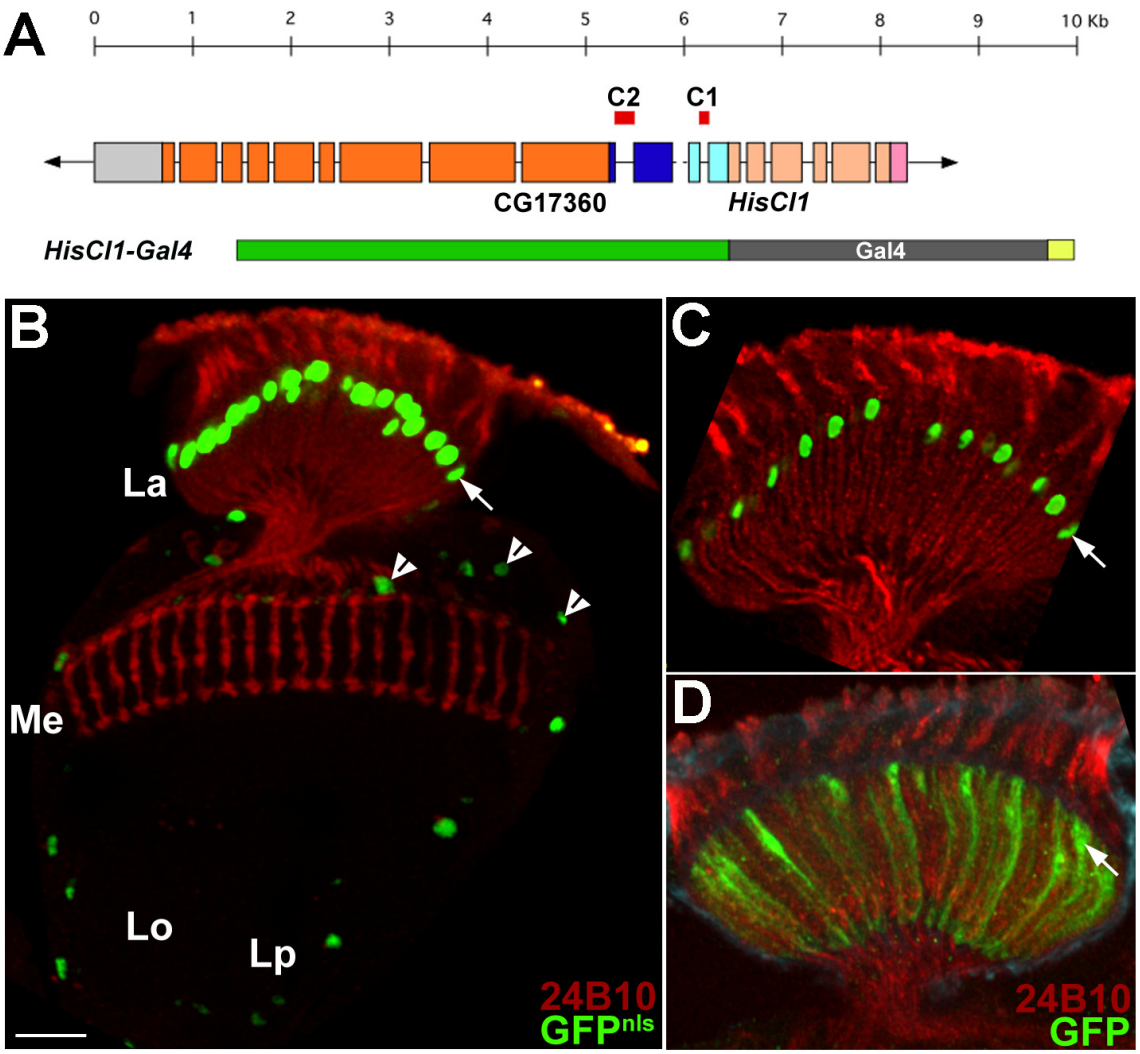
A
0
1
2
3
4
5
6
7
8
9
10 Kb
C2
C1
CG17360
HisCl1
HisCl1-Gal4
Gal4
B
La
Me
Lo
Lp
24B10
GFPnls
C
D
24B10
GFP

Figure S3. Histamine Chloride Channel 1 Is Expressed in Lamina Glia and Medulla Cells

(A) Promoter analysis of the *HisCl1* gene. The *HisCl1* genomic structure is shown as a linear cartoon: exons are indicated as boxes and introns and intergenic sequences as lines. Comparative genomic analysis identified two blocks of sequences (C1,C2; red boxes shown above the genomic structure) that are conserved in at least 11 out of 12 analyzed *Drosophila* species (see supplementary Figure 2). A large genomic region (green box) containing C1 and C2 as well as a part of the neighboring gene, *CG17360*, was fused to Gal4 (grey box) and *hs70* 3'UTR (yellow box) to generate the *HisCl1-Gal4* driver.

(B-D) Expression pattern of *HisCl1-Gal4* in the optic lobe. The *HisCl1-Gal4* was used to drive the expression of nuclear-tagged GFP (GFP^{nls}) (B,C) or cytoplasmic GFP (GFP) (D) markers (green). (C,D) High magnification views of the lamina. The HisCl1-Gal4 drives strong expression in lamina epithelial glia (arrows), with identifying nuclear locations in the distal lamina, which wrap around lamina cartridges (D). It is also expressed weakly in subsets of uncharacterized medulla cells (arrowheads) (B). Photoreceptors axons were visualized using MAb24B10 antibody (red).

Scale bar: in (B) 20 μm.

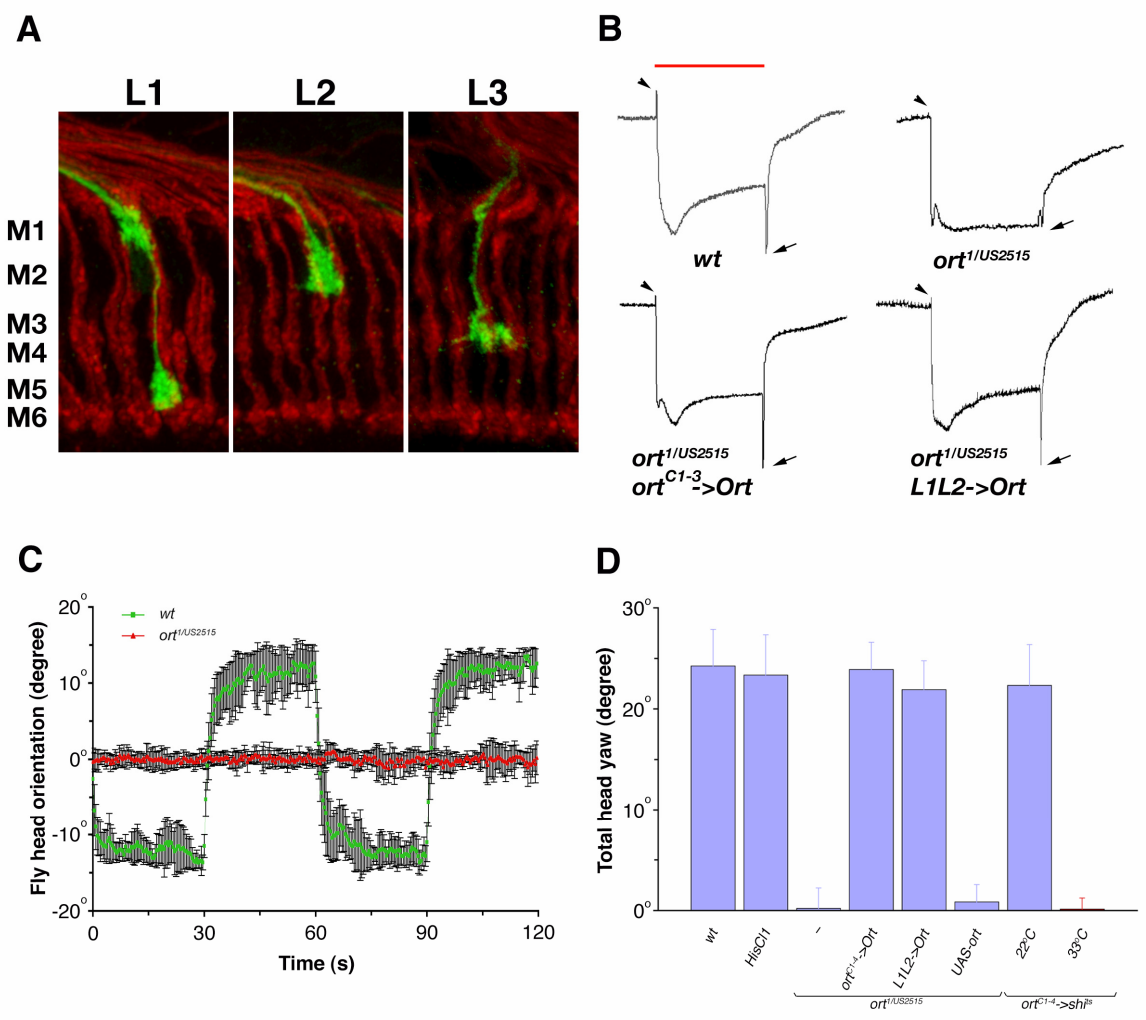
A
L1
L2
L3
M1
M2
M3
M4
M5
M6
B
wt
ort1/US2515
ort1/US2515
ortC1-3->Ort
ort1/US2515
L1L2->Ort
C
wt
ort1/US2515
Fly head orientation (degree)
20°
10°
0°
-10°
-20°
0
30
60
90
120
Time (s)
D
Total head yaw (degree)
30°
20°
10°
0°
wt
HisCl1
-
ortC1-4->Ort
L1L2->Ort
UAS-ort
22°C
33°C
ort1/US2515
ortC1-4->shits

Figure S4. The Histamine Chloride Channel Ort Is Expressed in the Lamina Neurons L1-L3 and Is Required for Motion Detection

(A) Axon terminals of L1, L2, and L3 mark different medulla strata. Single lamina L1-L3 neurons (green) were visualized using the *ort^{C1-3}-Gal4* driver and the genetic mosaic system (*hs-Flp/UAS>CD2>mCD8-GFP*, see text for details). L1 terminals arborize in medulla strata M1 and M5, while L2 and L3 terminate in strata M2 and M3, respectively. Photoreceptor axons were visualized with MAb24B10 antibody (red) to mark the M3 and M6 strata.

(B) Expressing Ort using the *ort^{C1-3}-Gal4* driver rescues electroretinogram (ERG) defects in *ort* mutants. The 'on'- (arrowheads) and 'off'-transients (arrows), which largely reflect the responses of lamina cells, were absent in *ort* mutants. Expressing Ort using the *ort^{C1-3}-Gal4* or *L1L2-Gal4* driver in *ort* mutant flies restored their 'on'- and 'off'-transients.

(C) Real-time head yaw optomotor responses measured in wild-type (green) and *ort* mutants (red). Motion stimuli were provided by a striped drum rotating in alternate directions for 30 sec per direction (see Experimental Procedures for details). Wild-type flies responded to the rotating striped drum with syndirectional head turning while *ort* mutants exhibited no significant response. Means of responses were plotted (in degrees of rotation; 0^o: initial head position; negative/positive: clockwise/counterclockwise rotation). Error bars (standard deviation): variations among 30 trials.

(D) Histogram of optomotor responses of wild-type and various *ort* mutants. *Ort,* but not *HisCl1*, mutants exhibited essentially no optomotor response. Expressing Ort using the *ort^{C1-4}-Gal4* or *L1L2-Gal4* driver rescued optomotor defects in *ort* mutants. Expressing *shi^{ts1}* using the *ort^{C1-4}-Gal4* driver abolishes flies' optomotor response at the restrictive, but not permissive, temperatures. Error bars indicate standard deviations.

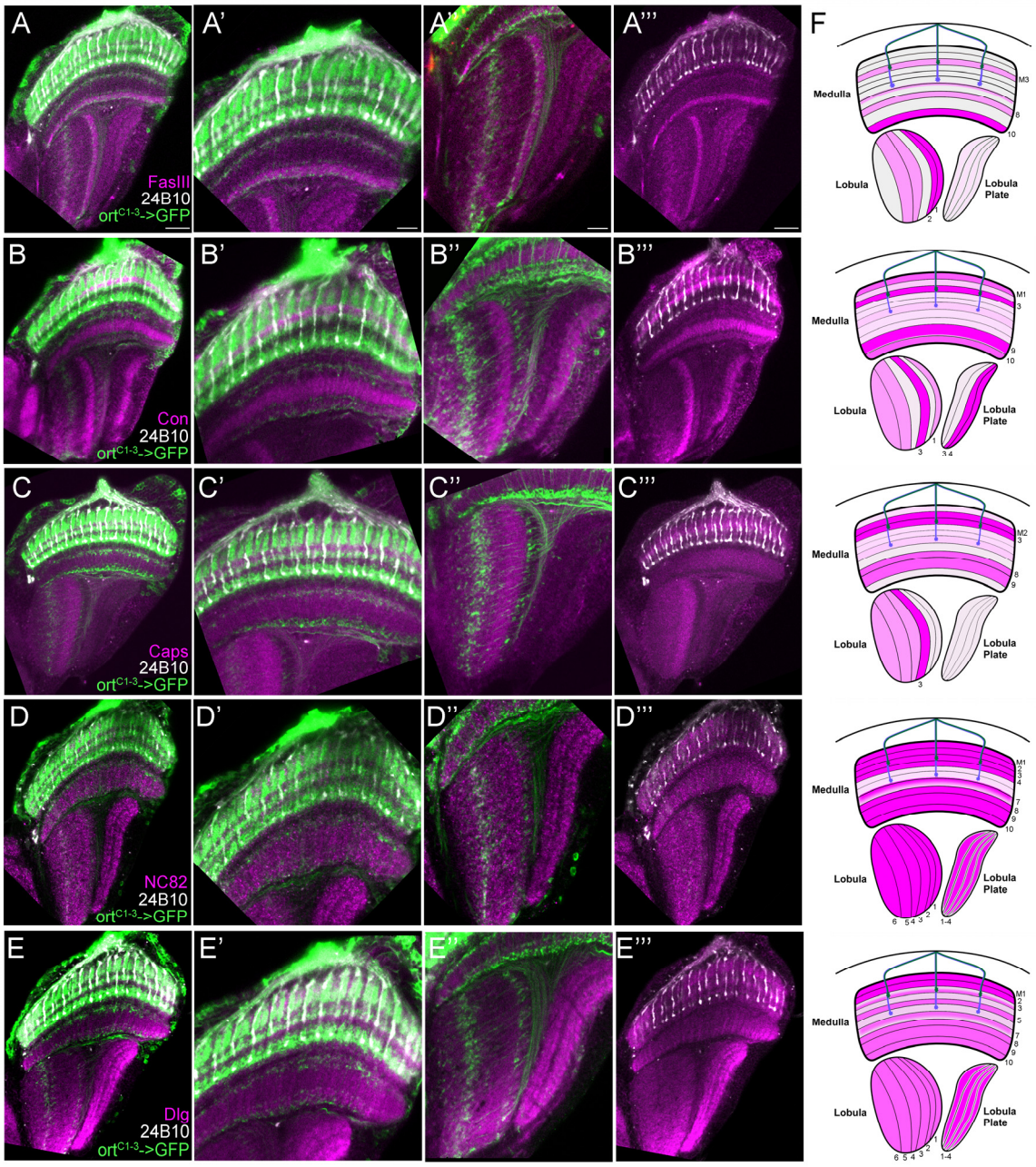
A
A'
A''
A'''
FasIII
24B10
ort^C1-3->GFP
B
B'
B''
B'''
Con
24B10
ort^C1-3->GFP
C
C'
C''
C'''
Caps
24B10
ort^C1-3->GFP
D
D'
D''
D'''
NC82
24B10
ort^C1-3->GFP
E
E'
E''
E'''
Dlg
24B10
ort^C1-3->GFP
F
Medulla
Lobula
Lobula Plate
M3
8
10
M1
3
9
10
M2
3
8
9
M1
2
3
4
7
8
9
10
1-4
5

Figure S5. Different Surface Receptors Label Distinct Medulla and Lobula Strata

(A-C) The expression patterns of three surface receptors, Fasciclin III (FasIII), Connectin (Con), and Capricious (Caps) in optic lobes examined by antibody labeling (magenta). (D-E) The antibodies against the presynaptic protein Bruchpilot (Brp/NC82) and postsynaptic marker Discs large (Dlg) were used to label the columnar and laminar structures of the optic lobes (magenta). Photoreceptor axons were labeled by MAb24B10 (white). Ort-expressing neurons were visualized using the $ort^{C1\text{-}3}$-LexA::VP16 driver and the LexAop-rCD2::GFP reporter (green). The following antibodies were labeled (magenta).

(A-A”’) Anti-FasIII immunolabeling.

(B-B”’) Anti-Con immunolabeling.

(C-C”’) Anti-Cap immunolabeling.

(D-D”’) nc82 immunolabeling.

(E-E”’) Anti-Dlg immunolabeling.

(A’-E’, A”-E”) High magnification views of (A-E), respectively.

(A”’-E”’) Green channel from Ort expressing neurons omitted from (A-E) to reveal the neuropil strata and photoreceptor terminals.

(F) Schematic representations of (A”’-E”’). Various saturation levels of magenta indicate the different expression levels of receptors and markers.

Scale bar: in (A), 20 μm for (A-E, A’’’-E’’’); in (A’), 10 μm for (A’-E’, A’’-E’’).

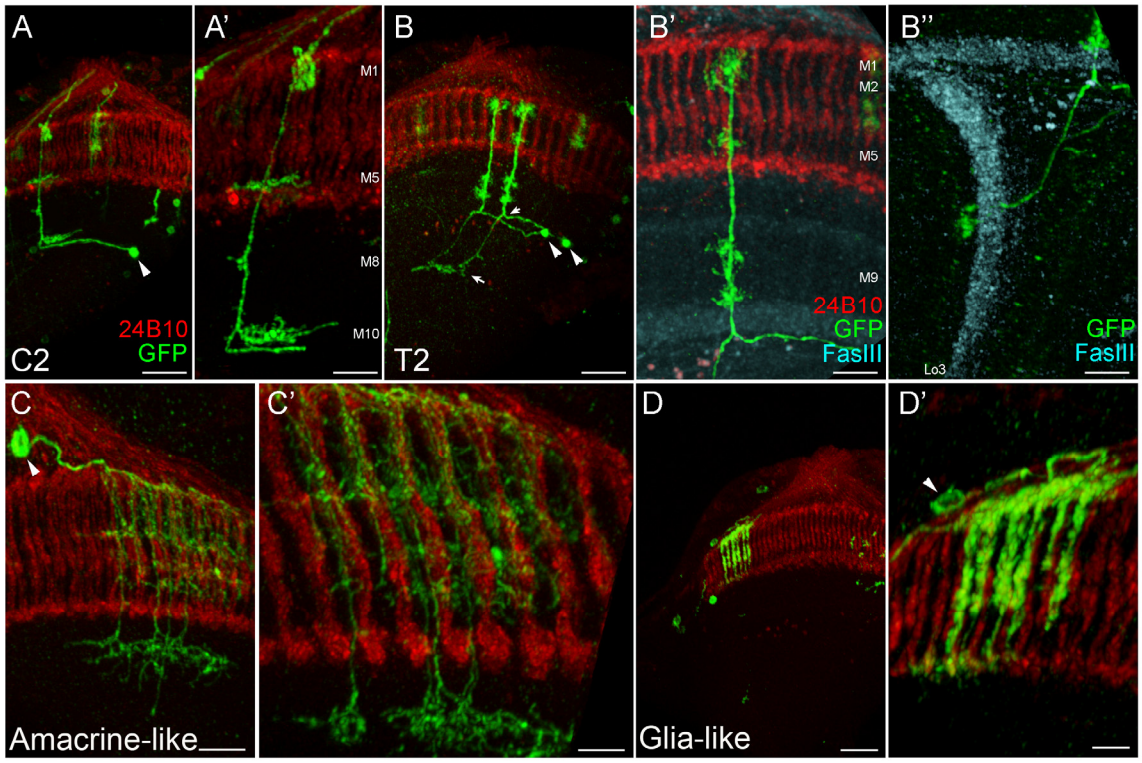
A
A'
B
B'
B''
M1
M5
M8
M10
M1
M2
M5
M9
24B10
GFP
C2
T2
24B10
GFP
FasIII
GFP
FasIII
Lo3
C
C'
D
D'
Amacrine-like
Glia-like

Figure S6. Ort Is Expressed in Centrifugal Neurons C2 and T2 as well as in Medulla Amacrine-Like and Glia-Like Cells

Single-neuron clones were generated using the flip-out mosaic system and labeled with the mCD8-GFP marker (green) as described in Figure 3. MAb24B10 (red) and anti-FasIII (cyan), labeling photoreceptors and specific strata respectively, serve as landmarks. The $ort^{C1\text{-}3}$-*Gal4* driver was expressed in two types of centrifugal neurons, C2 (A, A') and T2 (B-B"), with cell bodies (arrowheads) located in the lobula plate cortex (see Figure 1A).

(A, A') The C2 neuron projects axons through the medulla neuropil and terminates at the lamina (not shown). Its axon arborizes in medulla strata M1, M5 and M10.

(B-B") A pair of T2 neurons. Their axons bifurcate just beneath stratum M10 (small arrow): one branch terminates at lobula stratum Lo3 and the other arborizes at medulla strata M2, M5, and M9 and terminates at stratum M1.

The $ort^{C1\text{-}3}$-Gal4 driver also labeled at low frequency two novel medulla cells, designated amacrine-like and glia-like cells. The cell bodies are marked by arrowheads (C, D').

(C) The amacrine-like cell extends complex wide-field processes spanning multiple medulla columns.

(D) The glia-like cell has a soma in the cortex (arrowhead) and wraps around multiple columns containing photoreceptor terminals.

Scale Bar: in (A, B, D), 20 μm; in (A', B', B''), 8 μm; in (C), 10 μm; in (C', D'), 5 μm.

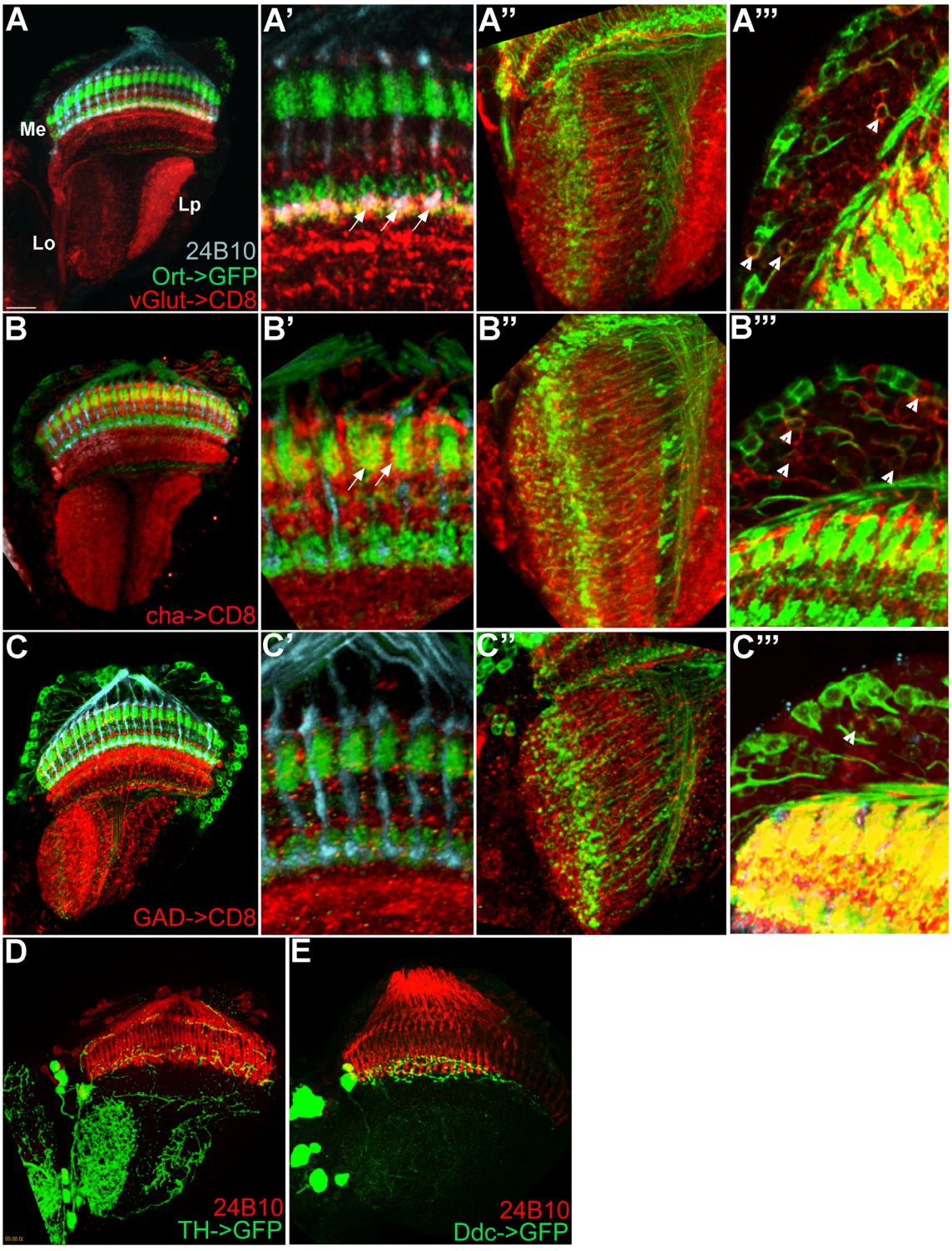
A
Me
Lp
Lo
24B10
Ort->GFP
vGlut->CD8
A'
A''
A'''
B
cha->CD8
B'
B''
B'''
C
GAD->CD8
C'
C''
C'''
D
24B10
TH->GFP
E
24B10
Ddc->GFP

Figure S7. Neurotransmitter Phenotype of Ort-Expressing Neurons Assessed Using Gal4 Lines

Neurotransmitter contents in Ort-expressing neurons was examined using a dual-expression system. (A-C”’) Ort-expressing neurons were labeled using $ort^{C1\text{-}3}$-*LexA::VP16* and *LexAop-rCD2::GFP* (green). Various Gal4 lines were used to express the CD8 marker (red) in neuron subsets that express different neurotransmitter phenotypes (see Experimental Procedures for details). Photoreceptor axons were labeled with MAb24B10 (cyan).

(A-A”’) The expression pattern of *vGlut-Gal4* (vesicular glutamate transporter), a phenotypic marker for glutamatergic neurons. Note that there is significant overlap between GFP and CD8 labeling in medulla stratum M6 (arrows, A’), which was likely brought about by the processes of Dm8 neurons. A number of cell bodies in the medulla cortex was marked with both GFP and CD8 (arrowheads, A”’).

(B-B”’) The *cha-Gal4* (choline acetyltransferase) expression pattern, a phenotypic marker for cholinergic neurons. Note that GFP and CD8 signals co-localize to stratum M2 (arrows, B’), likely brought about by the axon terminals of L2 neurons.

(C-C”’) The *GAD-Gal4* (glutamic acid decarboxylase I) expression pattern for GABAergic neurons. Minimal overlapping between GFP and CD8 labeling in the medulla neuropil (C’) and cortex (C”’) was found.

(D-E) Possible dopaminergic and serotonergic neurons were identified by using *TH-Gal4* and *Ddc-Gal4* to drive the expression of mCD8GFP marker (green). (D) The *TH-Gal4* (tyramine hydroxylase) expression pattern. (E) The *Ddc-Gal4* (DOPA decarboxylase) expression pattern. Both drivers labeled only tangential neurons in the medulla.

(A’-C’), (A”-C”), and (A”’-C”’) are high magnification views of the medulla, lobula, and medulla cortex of (A-C), respectively. Scale bar: 20 μm in (A) for (A-E).

References

Friggi-Grelin, F., Coulom, H., Meller, M., Gomez, D., Hirsh, J., and Birman, S. (2003). Targeted gene expression in Drosophila dopaminergic cells using regulatory sequences from tyrosine hydroxylase. J. Neurobiol. 54, 618–627.

Hong, S.T., Bang, S., Paik, D., Kang, J., Hwang, S., Jeon, K., Chun, B., Hyun, S., Lee, Y., and Kim, J. (2006). Histamine and its receptors modulate temperature-preference behaviors in Drosophila. J. Neurosci. 26, 7245–7256.

Mahr, A., and Aberle, H. (2006). The expression pattern of the Drosophila vesicular glutamate transporter: a marker protein for motoneurons and glutamatergic centers in the brain. Gene Expr. Patterns 6, 299–309.

Ng, M., Roorda, R.D., Lima, S.Q., Zemelman, B.V., Morcillo, P., and Miesenbock, G. (2002). Transmission of olfactory information between three populations of neurons in the antennal lobe of the fly. Neuron 36, 463–474.

Sepp, K.J., and Auld, V.J. (1999). Conversion of lacZ enhancer trap lines to GAL4 lines using targeted transposition in Drosophila melanogaster. Genetics 151, 1093–1101.

Yasuyama, K., Kitamoto, T., and Salvaterra, P.M. (1995). Localization of choline acetyltransferase-expressing neurons in the larval visual system of Drosophila melanogaster. Cell Tissue Res. 282, 193–202.